Non-classical Export of an Adenovirus Structural Protein

Lloyd C. Trotman[1) 2)], Dominik P. Achermann[1)], Stephan Keller, Monika Straub & Urs F. Greber[+)]

Zoologisches Institut der Universität Zürich, Winterthurerstrasse 190
CH-8057 Zürich, Switzerland

[1)] equal contributions

[2)] present address: Molecular and Developmental Biology, Memorial Sloan-Kettering Cancer Center, New York, USA

[+)] corresponding author:
Telephone: +41 1 635 4841
Fax: +41 1 635 6822
Email: ufgreber@zool.unizh.ch

Keywords: Adenovirus, extracellular protein gradient, non-classical protein export, penton base, protein delivery

Abbreviations: Ad: Adenovirus; ADP: Adenovirus death protein; BFA: brefeldin A; CLSM: confocal laser scanning microscopy; CMV: cytomegalovirus; DIC : differential interference contrast; Gal-T: galactosyl transferase; HIV: Human Immunodeficiency Virus; mAb: mouse monoclonal antibody; pAb: polyclonal rabbit antibody; Pb: penton base; PFA: para-formaldehyde; p.i.: post infection; p.t.: post transfection; PTD: protein transduction domain; ts1: temperature sensitive mutant 1; wt: wild type.

Title (characters including spaces)	56
Abstract: (words)	228
Total characters including spaces	51163

Abstract

The icosahedral capsids of Adenoviruses (Ads) consist of the hexon and stabilizing proteins building the facettes, and of the vertex protein penton base (Pb) anchoring the protruding fibers. The fibers bind to the Coxsackie virus B Ad cell surface receptor (CAR) and Pb to integrins. Here we describe a novel property of the Ad2 Pb. Pb was found to leave the infected cell and, upon exit, it attached to the surrounding noninfected cells forming a radial gradient with highest Pb levels on cells adjacent to the infected cell. The producer cells remained intact until at least 30 h post infection. At this point, Pb was not recovered from the extracellular medium suggesting that its cell-cell spread might not involve free Pb. When viral particles were released at late stages of infection, soluble Pb was found in the extracellular medium and it randomly bound to noninfected cells. Nonlytic export of Pb occurred upon transient transfection with plasmid DNA, but plasmid-encoded fiber was not exported, indicating that cell-cell spread of Pb is autonomous of infection. Pb export was not affected by Brefeldin A-induced disruption of the Golgi apparatus, suggesting that it occurred via a non-classical mechanism. Interestingly, the coexpression of Pb and fiber lead to both Pb and fiber export, termed ‘protein abduction’. We suggest that fiber abduction might support viral dissemination in infected tissues by interfering with tissue integrity.

Introduction

Secreted proteins generally contain a leader- or export sequence which directs their synthesis to the endoplasmic reticulum (ER). Typically, they are co-translationally inserted into the ER lumen by virtue of a signal sequence (1, 2), and are then transported towards the Golgi (3). In addition, secreted proteins lacking a classical signal sequence can be released in rare cases from mammalian cells, independent of an intact Golgi apparatus. Fibroblast growth factor (FGF) 1 and 2 (4), interleukin (IL) 1β (5) the human immunodeficiency virus-1 (HIV-1) transactivating protein TAT (6) and the Herpes virus structural protein VP22 (7) are examples of such proteins. IL-1β, FGF-1 and FGF-2 are secreted by a vesicular non-classical mechanism involving secretory lysosomes, and can be involved in the inflammatory response of hematopoietic cells (8). HIV-1 TAT and Rev, however, seem to be transported directly across the plasma membrane. The arginine and lysine-rich domains of HIV TAT and Rev, flock house virus capsid protein and the DNA binding segments of leucine zipper proteins, such as c-Fos and c-Jun as well as the yeast transcription factor GCN4 can interact with cellular membranes and translocate in a temperature independent but saturable process (9).

Many of the proteins that are exported by non-classical mechanisms can also be imported into cells, often by unconventional means, i.e., independent of endocytic uptake. HIV-1 TAT and VP22 are efficiently imported at 4° C in a process which has been termed protein transduction (10). The amino acid sequence requirements for transduction - the so called protein transduction domain (PTD) - have been identified for HIV1 TAT, Herpes simplex virus (HSV)-1 VP22 and the Drosophila antennapedia DNA-binding homeodomain (AntpHD). Proteins capable of transduction often contain regions that are rich in lysine and arginine residues which may assist association with negatively charged heparan sulfates or with phospholipids of the plasma membrane. Some of the identified PTD's have been genetically transferred to acceptor proteins and the resulting fusion proteins were, under certain conditions, able to spread across cell borders and into various tissues of living mice (11), demonstrating an interesting therapeutic potential of PTD's. In the case

of the AntpHD, a rather hydrophobic region of amino acids 41-58 in the third helix has been associated with the ability of the protein to cross membranes (12). This sequence is somewhat homologous to amino acids 160-167 of the Adenovirus type 2 (Ad2) capsid protein penton base (Pb), and it has been reported that exogenously added recombinant Pb is able to enter naïve cells (13).

Here, we tested if the native Ad2 capsid protein Pb is able to spread from a producing cell to neighboring cells. Ad2 belongs to the species C Ads and infects airway epithelial cells (14). A prominent component of the viral capsid is Pb, located at the icosahedral verteces as a homo-pentamer (15). Each pentamer anchors one copy of a trimeric fiber protein and this requires an interesting symmetry mismatch which has not yet been solved at atomic resolution. Fiber-Pb hetero-oligomers are formed in the cytosol during the synthesis of structural proteins, approximately 20 h p.i. and are then inserted into the nascent virion (for reviews, see 16, 17). Upon cell disruption, the large majority of virions are released. Extracellular particles bind via the globular fold of the C-terminal fiber head domain to the amino-terminal D1 domain of the Ad2 and Ad5 receptor, the Coxsackie B virus Adenovirus receptor (CAR, reviewed by 18). CAR is localized at tight junctions and the basolateral surface of polarized epithelial cells (19). It engages in homophilic contacts that are also used for fiber binding (20). Interestingly, fiber binding to CAR has recently been suggested to disrupt tight junctions of airway epithelial cells and help spread the infection to the apical side, but it is unknown if free fibers or virion-associated fibers are responsible for this process (21). Subsequent to binding of the virion-associated fiber to CAR, interactions of Pb with leucine-aspartate-valine (^{287}LDV) and arginine-glycine-aspartate (^{340}RGD) motives of alpha v and β3 or β5 integrins induce the release of the fibers from Pb (22) and promote viral internalization via clathrin-coated pits (23, 24). Pb interactions with integrins are also important for the lysis of pinosomal membranes (24). Our results now reveal an additional property of Pb, namely the promotion of its own export and also the export of fibers complexed to Pb. We have termed this process ‘protein abduction’ and suggest that it may promote viral spread in the infected tissue.

Results

Transiently transfected Pb is found on neighboring cells

To study the subcellular distribution of Pb we transiently transfected human lung carcinoma A549 cells with a eukaryotic Pb expression construct (SK5.5) using Lipofectamin. To our surprise, we found significant amounts of Pb on neighboring non-transfected cells as visualized by the polyclonal rabbit anti-Pb antibody R2 (pAb R2) 25 h post transfection (p.t.) (Fig. 1, a, a'). Pb was distributed in a radial gradient emanating from the cell expressing the plasmid. To test whether this phenomenon was dependent on the transfection method, cells were transfected using the $CaPO_4$ precipitation method or microinjected into the nucleus. Both procedures yielded the same result, albeit with a somewhat delayed phenotype in the case of $CaPO_4$, and clearest spreading results around 60 h p.t. (Fig. 1, b, b', and not shown). No gross changes of morphology were detected in Pb-expressing cells as suggested by differential interference contrast (DIC) microscopy (Fig. 1, a, b).

Cell to cell spreading of Pb occurs during adenoviral infection

To test whether the observed cell to cell spreading of Pb also occurred during Ad2 infection, A549 cells were infected with wt Ad2 at a low multiplicity of infection (MOI) and analyzed by indirect immunofluorescence using the Pb-specific R2 antibody. Consistent with a normal progression of Ad2 infections in these cells, Pb was found mainly in the nucleus at 15 and 20 h post infection (p.i.) (Fig. 2A, a-b'). At 25 h p.i., however, a significant fraction of the Pb signal was visible outside of the infected cells (c'), similar to cells transfected with the Pb plasmid DNA shown in Fig. 1. A similar staining pattern of Pb in the infected and the surrounding cells was detected with the monoclonal Pb-specific antibody pAb 591 (Fig. 2D). We then extended the analysis to different cell types showing that cell to cell spreading of Pb also occurred in human epidermoid carcinoma KB cells and HeLa cells at similar time points p.i. (Fig. 2B). When analyzing various Ad2 mutants (dl762, dl712, ts1) that all carry intact Pb genes, we observed that trafficking of the Pb

protein was never affected (Fig. 2C). dl712 is an Ad2/Ad5 hybrid virus with a deletion of the E3 Ad death protein (ADP, 25, 26) and the dl762 mutant has a deletion in the E3 14.7 K protein (27). Likewise, Ad2 ts1 bearing a point mutation in the L3/p23 protease gene which renders the protein incapable of packaging into newly synthesized virions at the restrictive temperature (28) clearly showed cell to cell spreading of its Pb protein. These observations confirm the above finding that the expression of Pb first leads to Pb accumulation in the cytoplasm and the nucleus and then also on the surrounding cells, independent of the presence of other viral proteins.

A major fraction of intact Pb is exported

We next tested if Pb was present in the extracellular medium. A549 cells were infected with Ad2 in protein-free medium and the supernatants were collected at different times up to 32 h p.i.. The medium was cleared by low speed centrifugation, acid precipitated and analyzed by Western blotting using the anti-Pb antibody R2 and an anti-interleukin (IL)-6 antibody (Fig. 3A). Pb was absent in all the supernatants comprising 10^5 cell equivalents each, but it was readily recovered from the infected cells. The pro-inflammatory cytokine IL-6 was recovered in the supernatants of both infected and noninfected cells, indicating that the cells were secretion competent. This supported the notion that IL-6 is released from cells upon stress induction, including viral insults (29-31). We attempted to recover Pb from the growth medium supplemented with BSA, but failed to collect Pb by immunoprecipitations and Western blotting from 10^5 cell equivalents (Fig. 3B). Pb was, however, recovered from the medium at 42 h p.i. when cell lysis had occurred (not shown). On Western blots, our detection limit was 0.1 µg of Pb and we immunoprecipitated about 1 µg of Pb from 10^5 cells extracted with freon at 70 h p.i. (32). Considering that each cell produces 10^4 virions (33), more than 99% of the cell-associated Pb must have been free, i.e., not assembled in particles. This suggests that less than 10% of the cell-associated Pb could have been released into the medium. We next tested if extracellular Pb was binding to noninfected cells using the immunofluorescence assay described in Figures 1 and 2. A549 cells were incubated with Ad2 in the cold (moi 10), and infected by warming in DMEM-containing BSA for 41 h. The medium was collected, centrifuged at 108'000 x g for

1 h to pellet virus particles, and the supernatant was added to noninfected A549 cells for 6 h at 37°C. Pb immunoreactivity of fixed specimens was detected around the periphery of all the cells on the coverslip, but cells incubated with medium from noninfected cells were negative for Pb immunoreactivity, except for mitotic cells with nonspecific stainings of the secondary antibodies (Fig. 3C, panels d-i). The Pb staining of infected medium on interphase cells was indistinguishable from the Pb staining detected in radial gradients around infected cells (see Figures 1 and 2). It is of note that this Pb staining was mainly peripheral (see also Fig. 7). In contrast, Pb of purified Ad2 particles was present in both the cytoplasm and around the nucleus at 6 h p.i., indicative of viral entry and Pb delivery to the cytosol (Fig. 3C, panels a-c).

We also tested if Pb was passed through the filters of a TransWell (Becton Dickinson, Switzerland). A 95% confluent monolayer of A549 cells grown on membrane filters with pore sizes of 1 and 3 µm, respectively, was infected with Ad2 at moi 100 for 2 h, washed and the filters placed on noninfected acceptor cells on glass coverslips for up to 44 h p.i.. No signs of Pb spreading to the acceptor cells were found up to 20 h p.i., but the first infected acceptor cells were scored at 20 h p.i. by strong Pb and fiber stainings in the nucleus (not shown). At 44 h p.i., Pb was found across the surface of essentially all the acceptor cells, and many cells were infected, suggests that the observed Pb spreading on these cells could be due to Pb from the filter based cells and / or the infected acceptor cells (not shown). Together, all these data argue that Pb is nondetectable in the medium up to about 30 h p.i., when significant Pb spreading around the infected cells is observed. At later time points, Pb spreads more randomly to noninfected cells and is also found in the extracellular medium.

To quantify the amounts of Pb protein exported from an infected cell to the neighboring cells prior to viral release, Ad2-infected cells were fixed 30 h p.i. and immunostained for Pb using pAb R2. The signal intensities were quantified both inside and outside of the infected cell. Figure 4 A shows an example of this analysis including the areas defined for quantification. Our measurements showed that 46.6% (n=18, Stdev = 13.7%) of the Pb signal was located outside of the infected cell. To determine if Pb was intact or

fragmented, A549 cells were transfected with the Pb expressing plasmid DNA (SK5.5). The cell monolayers were lysed at various time points p.t. and the lysates analyzed for Pb by SDS-PAGE (Fig. 4B, a) and Western blotting (b) using the pAb R2. No degradation products were detected in this experiment, demonstrating that the exported R2 epitopes of Pb were largely intact. We concluded that less than 10% of Pb produced at 31 h p.i. is present in the medium but more than 40% of the cell associated PB is picked up by the neighboring cells.

Pb leaves intact cells by a Golgi-independent mechanism

To gain insight into the mechanism of Pb export from the producing cell we first tested whether Pb-expressing cells were generally more permeable due to a lysogenic effects of viral proteins. To assess cell integrity, we used Trypan Blue which readily diffuses into the nucleus of permeabilized cells. Infected cells were identified by the expression of eGFP from recombinant Ad5 lacking the E1 region (Ad5-eGFP). 911 cells contain stably integrated adenoviral E1 genes (34) and are thus permissive for production of Ad5-eGFP particles. At 30 h p.i. eGFP-expressing cells were never Trypan Blue positive, although Trypan Blue positive cells were occasionally detected as shown in Fig. 5A (arrows). This strongly suggests that the plasma membrane of infected cells was not permeabilized at this time point. Cells were then fixed, permeabilized and processed for immunofluorescence with the pAb R2. Pb was seen outside of infected cells, demonstrating that the Pb protein of Ad5-eGFP is capable of spreading from an apparently intact cell to neighboring cells (Fig. 5B). This finding confirmed the result obtained by infection of cells with the Ad2 deletion mutant dl712, which lacks the ADP gene. Using the Trypan Blue assay, dl712 had been found to lyse cells no earlier than 120 to 140 h p.i. (26), but we observed cell to cell spreading of Pb as early as 25 h p.i.. To test whether Pb export required a functional Golgi apparatus, the Golgi apparatus was disrupted by Brefeldin A (BFA), which inhibits the GDP-GTP exchange factor of the ADP-ribosylation factor (ARF) 1 in Golgi membranes (35). This causes an inhibition of classical export (36). A549 cells were transiently transfected with Pb plasmid DNA or infected with wt Ad2 for 18 h. At this time point, Pb was detected in the transfected or infected cells but not in

neighboring cells (Fig. 5C, a', c'). The structure of the Golgi apparatus was clearly visible as indicated by indirect immunofluorescence using an antibody against galactosyl-transferase (Gal-T) (Fig. 5C, a'', c''). BFA was added to parallel samples and Pb export monitored 12 h later. As depicted in Fig. 5C (panels b'' and d'') the Golgi apparatus of BFA-treated cells disappeared and a diffuse background staining of Gal-T remained. Nevertheless, Pb protein was exported after transfection (b') and also after infection (d'). These findings are consistent with the lack of an obvious export sequence in Pb. Noteably, the pattern of Pb staining in the cells surrounding the transfected or infected cell was indifferent from the addition of BFA. This suggests that disruption of membrane traffic has apparently no effect on the location of Pb in the recipient cells. We also observed that cell to cell spreading of Pb was not affected by performing the transfection and spreading at 20° C (not shown), i.e., at conditions which block the export of newly synthesized secretory proteins in the Golgi apparatus (37). Our results therefore strongly suggest that Pb export does not require a functional secretory pathway and occurs by a non-classical mechanism.

Pb expressing cells mediate Ad2 fiber export

Next we examined whether other adenoviral proteins were also exported during infection. As summarized in Fig. 6A, we found that the Ad2 fiber protein but not the hexon protein was released from infected A549 cells. Spreading of fiber from cell to cell was also observed in HeLa and KB cells, but only in infected cells never in transfected cells expressing fiber protein alone, as shown in Fig. 6B (a, a'). Since fiber is known to assemble with coexpressed Pb both in infected and transfected cells (38, 39) and fiber is associated with Pb in the intact viral particle (40) we tested if coexpression of fiber and Pb was sufficient for spreading of fiber. A549 cells were cotransfected with fiber and Pb encoding plasmid DNA and cells were simultaneously stained for fiber and Pb with monospecific antibodies. As depicted in Fig. 6B (b, b', b'') the presence of Pb rescued the fiber spreading phenotype observed in the wt Ad2 infections, strongly suggesting that fiber spreading is directly mediated by Pb. To probe the subcellular localization of Pb and fiber after exiting the transfected cell, we analyzed the immunostainings of fiber and Pb by

confocal laser scanning microscopy (CLSM). Single optical sections near the bottom of the transfected donor cells indicated a cytoplasmic staining pattern of Pb (Fig. 7, a, green) and also fiber (Fig. 7, b, red), excluding the nucleus. In contrast, the surrounding cells had a granulated peripheral pattern of both Pb and fiber and this pattern mostly colocalized, as indicated by the yellow color in the merged images (Fig. 7, c). Scanning across the entire z-dimension further indicated that most of the Pb and fiber proteins were in the periphery of the acceptor cells but never in the nucleus (Fig. 7, d). Together, these results establish that Pb alone or together with fiber exits the cell where it was synthesized and attaches to the surface of neighboring cells in a radial concentration gradient. It does not seem to cross the membranes of the recipient cells.

Discussion

Our results show that Pb of Ad2 accumulates in a radial gradient on tightly packed cells around a producing cell of a monolayer. This phenomenon occurs in Ad2-infected and also in Pb-transfected cells. The first indication of Pb spreading was detected 20 h p.i. and Pb spreading increased with time, reaching up to 46 % of the newly synthesized Pb at 30 h p.i.. Less than 10% of the cell-associated Pb were present in the medium at this point and the producing cells were intact. Pb export to neighboring cells occurred in the presence of BFA, a specific inhibitor of the guanine nucleotide exchange factor of Golgi-resident ARF proteins, and also in cells incubated at 20° C blocking the formation of transport vesicles at the trans Golgi network (41). This suggests that Pb is released from the producing cell in a non-classical manner bypassing the secretory pathway. At later points of infection, i.e. when Ad particles are released to the medium and extracellular Pb-binding sites become saturated, Pb was recovered from the medium and found on all the noninfected cells. This argues that Pb initially passes from the infected cell to neighboring cells without its extended presence in the medium.

In contrast to TAT and also VP22, the released Pb is predominantly found on the surface and perhaps in cytoplasmic vesicles of recipient cells rather than in the cytosol and the nucleus. This illustrates that a fraction of Pb may be handed over to endocytic receptors, such as alpha v integrins. Importantly, Pb alone (or in combination with fiber) was apparently not sufficient for penetration of the plasma membrane of naïve cells. This observation is consistent with the notion that the endosomolytic activity of species C Ads requires the viral capsid and also viral signalling rather than isolated capsid components alone (24, 31, 42). It is interesting to note that recombinant Pb isolated from insect cells bound and also internalized into cultured human epithelial cells (13). A fraction of Pb was even found inside the nucleus, although most of it was degraded 4 h after addition to the cell monolayer. It was suggested that one function of this unusual behaviour might be to help targeting the incoming Ad particle to the nucleus. Although this is in principle conceivable, it is unlikely that Pb has a dominant role in docking the Ad particle to the nuclear membrane. It was recently shown that the binding of intact Ad2 to isolated nuclear envelopes was abolished by the addition of isolated hexon proteins and was only weakly inhibited by the addition of an excess of Pb purified from infected cells (43). In addition, analysis of the stepwise uncoating process of incoming Ad2 had demonstrated earlier that approximately 70 % of the Pb dissociated from the virion before the particle attached to the nuclear pore complex (32). A potential role of Pb in attaching the viral particles to the nuclear pore complex is thus unlikely, although not completely excluded. Whether the reported nuclear targeting of the recombinant Pb has any *in vivo* relevance or if it is a speciality of the recombinant Pb or represents a different mechanism of accessing the target cells is presently unknown. Interestingly and in contrast to the recombinant protein, the Pb protein produced in mammalian cells was stable for at least 69 h and more than 40 % of it was spread to recipient cells. Nonetheless, we have not observed any signs of Pb toxicity, in agreement with earlier reports (13, 23).

The mechanism of Pb spreading is complicated by the fact that Pb is a relatively large pentameric protein of 63.3 kDa and Pb mutagenesis has proven to have multiple effects on protein expression, folding and assembly (44). More information about possible mechanisms of protein transduction is, however, available from the small HIV TAT protein

that was discovered nearly 15 years ago (45, 46). The TAT PTD has an alpha helical character with basic residues making up one side of the alpha helix (47). The arginine / lysine-rich PTD's seem to require electrostatic interactions with negatively charged heparan sulfate proteoglycans or phospholipids (48), but it is unknown if the transduction process requires a denaturation step to expose the PTD or involves another type of activation (49).

In addition to spreading from the infected cell to neighboring cells, Pb has the potential to release another structural Ad protein, the fiber protein. Conceivably, spreading of Pb and fibers can block the receptors of the infected and the neighboring cells and thus help viral dissemination to more distant cells. In the context of polarized epithelial cells, fiber spreading to the extracellular medium might even help to dissolve tight junctions, as has been suggested to occur in airway epithelial cell infections (21). This process might be of significance also to other viral infections, e.g., for reovirus infections occurring through the junction associated molecule JAM (50). Obviously, Pb-fiber mediated dissociation of junctions would require a strict timing of Pb-fiber release. Pb would have to leave a cell before the newly synthesized particles exit, i.e. before the infected cell is lysed. Indeed, we observed that both Pb and fiber were only exported at detectable levels, if their concentration inside the producer cell was very high, e.g., at the time of ongoing capsid assembly. It is tempting to speculate that the overproduction of capsid proteins may not only drive the capsid assembly process (51) but also deliver an excess of crucial structural proteins to the surrounding cells and there, work in favour of the viral infection. Alternative or additional functions of Pb spreading could include signalling in surrounding cells to prepare them for infection, e.g., inducing the cell cycle which is particularly important in the case of non-dividing cells of tissues. Pb ligation of integrins could, e.g., activate the MAP kinase pathway and activate protein kinase A which are known to be triggered by the incoming Ad in an integrin-dependent manner (52, 53). An additional but more speculative function of released Pb and fiber proteins might be a local protection of the emerging viral particles from neutralizing host antibodies. A Pb-fiber complex might, for example, be particularly helpful to decoy circulating antibodies. In any case, it is not known, how robust the putative carrier function of Pb is, and it seems that recombinant gold-tagged Pb is not

able to break out of endosomes (13). Given that a biological role of any known PTD is so far missing, this suggests that the identification of the Pb PTD will not only broaden the versatility of Pb-mediated abduction but also shed more light on the mechanism of tight junction disruption in viral infections.

Acknowledgement

We thank Dr.'s E. Berger and H. Büeler (University of Zürich, Switzerland), P. Boulanger (University of Lyon, France), J. Chroboczek (Institut de Biologie Structural, Grenoble, France), E. Harlow (Massachusetts General Hospital, Charlestown, MA, USA), M. Horwitz (Albert Einstein College of Medicine, New York, USA) and W. Wold (University School of Medicine, St. Louis, USA) for gifts of antibodies and viruses, and Dr.'s T. Bächi and R. Stidwill (University of Zürich, Switzerland) for help with CLSM imaging. UFG was supported by funds from the Swiss National Science Foundation and the Kanton Zürich.

Methods

Cells and drugs

HeLa cells (human cervical epitheloid carcinoma), A549 cells (human lung carcinoma), KB cells (human epidermoid carcinoma of the mouth) and 911 cells (human embryonic retinoblasts, 34) were cultured in Dulbecco's modified Eagle's medium (DMEM, Gibco-BRL, Switzerland) containing 7% Clone III serum or 7% fetal bovine serum (FBS) (Hyclone, Integra BioSciences AG, Switzerland), 1% non-essential amino acids, 1% glutamine (Gibco-BRL, Switzerland). Alternatively, cells were also maintained in protein-free Turbodoma medium (Cell Culture Technologies, Bellinzona, Switzerland). Export experiments were performed with nearly confluent cells grown on 12 mm cover slips (54). Brefeldin A (Fluka, Switzerland) was used at 2.5 □g/ml and added to cells at 18 h p.i..

Viruses

Wt Ad2 was isolated from KB cells as described (32, 55), ts1-Ad2 (a temperature sensitive virus lacking the p23 protease, 56) was produced as described (57) and Ad5-eGFP (with deleted E1A and E1B regions and inserted eGFP controlled by the major cytomegalovirus (CMV) promotor) was a gift from H. Büeler (University of Zürich). Ad2 dl712 bearing a deletion in the E3 ADP gene and Ad2 dl762 with a deletion in the E3 14.7 K protein were obtained from W. Wold (26).

Antibodies

The mouse monoclonal antibody M73 against E1A proteins was received from E. Harlow (58) and the rabbit sera anti-Pb (R2), anti-hexon (R70), anti-fiber (R72) and anti-fiber plus Pb (R73) were gifts from M. Horwitz (59). The mouse monoclonal antibody 6A4 against fiber was obtained from J. Chrobockek (60), the rabbit anti-Pb antibody 591 was from P. Boulanger (39) and the mouse anti-Gal-T antibody was from E. Berger (University of

Zürich, 61). The rat anti-IL-6 antibody was purchased from Pharmingen (Becton Dickinson, Switzerland) and used at 1 µg/ml. Goat anti-mouse and goat anti-rabbit antibodies were conjugated to fluorescein-isothiocyanate or TexasRed (Sigma, Switzerland).

Plasmids, transfections and infections

The Pb expression plasmid SK5.5 (CMV-T7) was constructed by cutting pGMAd2PbFL571 with Bgl2 and ligating the insert into the BamH1 sites of pSCT2+ (54). The fiber expression plasmid SK6.10 (CMV-T7) was constructed by cutting pBKIIKS-Ad2 with Kpn1 followed by ligation of the insert into pSCT2+. Genomic sequences of Ad2 Pb and fiber were kindly supplied by Dr. P. Boulanger (Lyon, France). To assess Pb spreading, cells were grown to 80-95% confluency, Ad2 (1.5×10^6 PFU/ml) bound in the cold for 90 min in RPMI-0.2% BSA medium and internalized at 37° C in a CO_2 incubator as described (62). Under these conditions about 3 % of the input virus bound to cells (53). Cells were further incubated in growth medium containing FBS and analyzed as described. For transfections plasmids, Lipofectamin (5 µl / µg DNA, GibcoBRL, Life Technologies) and DMEM were incubated for 20 min at RT and than added to 90-95% confluent cells. After 3 h the cells were washed and growth medium was added. For $CaPO_4$ precipitation 1.5 µg DNA (for 5 cover slips) were diluted in 42 µl sterile H_2O, vortexed after addition of 5 µl 2.5 M $CaCl_2$, supplied with 50 µl Hepes-buffered saline and vortexed again. After incubation for 20 min at room temperature, 20 µl of DNA suspension were added to each coverslip, incubated for 24 h and supplied with fresh growth medium.

Immunofluorescence and microscopy

Transfected or infected cells were fixed with 3% PFA in PBS, permeabilized with 0.5% Triton X-100/PBS for 5 min and processed for indirect immunofluorescence. The coverslips were mounted in 0.5% para-phenylenediamine-80 % glycerol-20 mMTris (pH 8.8) and analyzed on a Reichert-Jung Polyvar microscope (Merk, Switzerland) equipped with DIC optics, a Texas Red (excitation filter 530 to 585 nm, long pass emission filter 615)

and a fluorescein filter set (excitation filter 475–495 nm, band pass emission filter 520–560) linked to a Charge Coupled Device video camera (Hamamatsu C5405, Hamamatsu Photonics, Germany) as described (62). CLSM images were acquired as described (24, 54, 55) using a pinhole setting corresponding to an optical thickness of approximately 0.5 µm.

Quantification of Pb release

Images were recorded with an electronically controlled inverted fluorescence microscope (Leica DM IRBE B) equipped with a Leica 63 x oil immersion objective (numeric aperature 1.32), a DIC polarizer, fluorescein and Texas Red excitation and emission filters (55). Fluorescence images were acquired using a digital, backilluminated charged coupled device camera in 16 bit recording mode (Princeton Instruments, Visitron Inc., Puchheim, Germany) and the MetaMorph software package (Universal Imaging Inc., Visitron Inc., Puchheim, Germany) as described (53). Intensity and area of a entire frame (800 □ 1000 pixels, 15 □m □ 15 □m / pixel), including the signals of the spreading Pb and of the primary infected cell were measured. The area (A in formula below) of the primary infected cell was determined by the DIC image, and the lowest pixel value in this region was chosen as a threshold value. Pixels with larger values than threshold were used to confirm the area of the primary infected cell. Background values were measured in a distal area of the image and the percentage of released Pb was calculated with the formula:

$$I_p = 1 - \frac{\left(I_{total} / A_{total} - I_{background} / A_{background}\right) \cdot A_{total}}{\left(I_{1^\circ cell} / A_{1^\circ cell} - I_{background} / A_{background}\right) \cdot A_{1^\circ cell}}$$

Ip = integrated pixel intensity over the area outside of the primary infected cell

I_{total} / A_{total} = averaged pixel intensity over the entire frame

$I_{background} / A_{background}$ = averaged pixel intensity of the background area

$I_{1° cell}$ / $A_{1° cell}$ = averaged pixel intensity of the primary infected cell

SDS PAGE and Western blot analysis

A549 cells were seeded on to 35mm dishes two days before the transfection and 80 % confluent cell layers were transfected by Lipofectamin , washed once with PBS and lysed with 300 l of boiling 1% SDS in H_20. The lysate was passed 5 times through a 22-gauge needle, boiled for 2 min, centrifuged in a table top centrifuge at maximum speed and mixed with an equal volume of 2 SDS sample buffer containing 20 mM fresh DTT. 25l were applied to a 10-15% polyacrylamide SDS-gel. Western blotting was performed with the primary antibody R2 (1:1000 dilution in 5% dry milk) against Pb and visualized by a horseradish peroxidase-linked secondary antibody using the enhanced Chemiluminescence (ECL) detection reagents as recommended by the manufacturer (Amersham-Pharmacia).

References

1. Lingappa VR, Shields D, Woo SL, Blobel G. Nascent chicken ovalbumin contains the functional equivalent of a signal sequence. J Cell Biol 1978;79(2 Pt 1):567-72.

2. Dobberstein B, Garoff H, Warren G, Robinson PJ. Cell-free synthesis and membrane insertion of mouse H-2Dd histocompatibility antigen and beta 2-microglobulin. Cell 1979;17(4):759-69.

3. Mellman I, Warren G. The road taken: past and future foundations of membrane traffic. Cell 2000;100(1):99-112.

4. Jackson A, Friedman S, Zhan X, Engleka KA, Forough R, Maciag T. Heat shock induces the release of fibroblast growth factor 1 from NIH 3T3 cells. Proc Natl Acad Sci U S A 1992;89(22):10691-5.

5. Rubartelli A, Cozzolino F, Talio M, Sitia R. A novel secretory pathway for interleukin-1 beta, a protein lacking a signal sequence. Embo J 1990;9(5):1503-10.

6. Ensoli B, Buonaguro L, Barillari G, Fiorelli V, Gendelman R, Morgan RA, et al. Release, uptake, and effects of extracellular human immunodeficiency virus type 1 Tat protein on cell growth and viral transactivation. J Virol 1993;67(1):277-87.

7. Elliott G, O'Hare P. Intercellular Trafficking and Protein Delivery By a Herpesvirus Structural Protein. Cell 1997;88(2):223-233.

8. Cleves AE. Protein transport: the nonclassical ins and outs. Curr. Biol. 1997;7:R318-R320.

9. Futaki S, Suzuki T, Ohashi W, Yagami T, Tanaka S, Ueda K, et al. Arginine-rich peptides. An abundant source of membrane-permeable peptides having potential as carriers for intracellular protein delivery. J Biol Chem 2001;276(8):5836-40.

10. Schwarze SR, Hruska KA, Dowdy SF. Protein transduction: unrestricted delivery into all cells? Trends Cell Biol 2000;10(7):290-5.

11. Schwarze SR, Ho A, Vocero-Akbani A, Dowdy SF. In vivo protein transduction: delivery of a biologically active protein into the mouse. Science 1999;285(5433):1569-72.

12. Derossi D, Joliot AH, Chassaing G, Prochiantz A. The third helix of the Antennapedia homeodomain translocates through biological membranes. J Biol Chem 1994;269(14):10444-50.

13. Hong SS, Gay B, Karayan L, Dabauvalle MC, Boulanger P. Cellular uptake and nuclear delivery of recombinant adenovirus penton base. Virology 1999;262(1):163-77.

14. Horwitz MS. Adenoviruses. In: Fields BN, Knipe DM, Howley PM, editors. Fields Virology. 3 ed. Philadelphia, Pa: Raven Press; 1996. p. 2149-2171.

15. Burnett RM. The structure of adenovirus. In: Chiu W, Burnett RM, Garcea RL, editors. Structural biology of viruses. Oxford: Oxford Press; 1997. p. 209-238.

16. Greber UF. Virus assembly and disassembly: the adenovirus cysteine protease as a trigger factor. Rev. Med. Virol. 1998;8:213-222.

17. Russell WC. Update on adenovirus and its vectors. J Gen Virol 2000;81(Pt 11):2573-604.

18. Wickham TJ. Targeting adenovirus. Gene Ther 2000;7(2):110-4.

19. Cohen CJ, Shieh JT, Pickles RJ, Okegawa T, Hsieh JT, Bergelson JM. The coxsackievirus and adenovirus receptor is a transmembrane component of the tight junction. Proc Natl Acad Sci U S A 2001;98(26):15191-6.

20. van Raaij MJ, Chouin E, van der Zandt H, Bergelson JM, Cusack S. Dimeric structure of the coxsackievirus and adenovirus receptor D1 domain at 1.7 A resolution. Structure Fold Des 2000;8(11):1147-55.

21. Walters RW, Freimuth P, Moninger TO, Ganske I, Zabner J, Welsh MJ. Adenovirus fiber disrupts CAR-mediated intercellular adhesion allowing virus escape. Cell 2002;110(6):789-799.

22. Nakano MY, Boucke K, Suomalainen M, Stidwill RP, Greber UF. The first step of adenovirus type 2 disassembly occurs at the cell surface, independently of endocytosis and escape to the cytosol. J Virol 2000;74(15):7085-95.

23. Nemerow GR, Stewart PL. Role of alpha(v) integrins in adenovirus cell entry and gene delivery. Microbiol Mol Biol Rev 1999;63(3):725-34.

24. Meier O, Boucke K, Vig S, Keller S, Stidwill RP, Hemmi S, et al. Adenovirus triggers macropinocytosis and endosomal leakage together with its clathrin mediated uptake. J. Cell Biol. 2002;158(6):1119-1131.

25. Deutscher SL, Bhat BM, Pursley MH, Cladaras C, Wold WS. Novel deletion mutants that enhance a distant upstream 5' splice in the E3 transcription unit of adenovirus 2. Nucleic Acids Res 1985;13(16):5771-88.

26. Tollefson AE, Scaria A, Hermiston TW, Ryerse JS, Wold LJ, Wold WS. The adenovirus death protein (E3-11.6K) is required at very late stages of infection for efficient cell lysis and release of adenovirus from infected cells. J Virol 1996;70(4):2296-306.

27. Brady HA, Scaria A, Wold WS. Map of cis-acting sequences that determine alternative pre-mRNA processing in the E3 complex transcription unit of adenovirus. J Virol 1992;66(10):5914-23.

28. Rancourt C, Keyvaniamineh H, Sircar S, Labrecque P, Weber JM. Proline 137 is critical for adenovirus protease encapsidation and activation but not enzyme activity. Virol. 1995;209(1):167-173.

29. Mann DL. Stress activated cytokines and the heart. Cytokine Growth Factor Rev 1996;7(4):341-54.

30. Balter M. Gene therapy on trial. Science 2000;288(5468):951-7.

31. Greber UF. Signalling in viral entry. Cell Mol Life Sci 2002;59:608-626.

32. Greber UF, Willetts M, Webster P, Helenius A. Stepwise dismantling of adenovirus 2 during entry into cells. Cell 1993;75:477-486.

33. Shenk T. Adenoviridae. In: Knipe DM, Howley PM, editors. Fundamental Virology. 4 ed. Philadelphia: Lippincott-Raven; 2001. p. 1053-1088.

34. Fallaux FJ, Kranenburg O, Cramer SJ, Houweling A, Van Ormondt H, Hoeben RC, et al. Characterization of 911: a new helper cell line for the titration and propagation of early region 1-deleted adenoviral vectors. Hum Gene Ther 1996;7(2):215-22.

35. Donaldson JG, Finazzi D, Klausner RD. Brefeldin A inhibits Golgi membrane-catalysed exchange of guanine nucleotide onto ARF protein. Nature 1992;360(6402):350-2.

36. Klausner RD, Donaldson JG, Lippincott-Schwartz J. Brefeldin A: insights into the control of membrane traffic and organelle structure. J Cell Biol 1992;116(5):1071-80.

37. Pepperkok R, Scheel J, Horstmann H, Hauri HP, Griffiths G, Kreis TE. Beta-COP is essential for biosynthetic membrane transport from the endoplasmic reticulum to the Golgi complex in vivo. Cell 1993;74(1):71-82.

38. Boudin M-L, Boulanger P. Assembly of adenovirus penton base and fiber. Virology 1982;116:589-604.

39. Karayan L, Gay B, Gerfaux J, Boulanger PA. Oligomerization of recombinant penton base of adenovirus type 2 and its assembly with fiber in baculovirus-infected cells. Virology 1994;202(2):782-95.

40. van Oostrum J, Burnett RM. Molecular composition of the adenovirus type 2 virion. J. Virol. 1985;56:439-448.

41. Griffiths G, Pfeiffer S, Simons K, Matlin K. Exit of newly synthesized membrane proteins from the trans cisterna of the Golgi complex to the plasma membrane. J Cell Biol 1985;101(3):949-64.

42. Seth P. Mechanism of adenovirus-mediated endosome lysis: role of the intact adenovirus capsid structure. Biochem. Biophys. Res. Commun. 1994;205(2):1318-1324.

43. Trotman LC, Mosberger N, Fornerod M, Stidwill RP, Greber UF. Import of adenovirus DNA involves the nuclear pore complex receptor CAN/Nup214 and histone H1. Nature Cell Biology 2001;3:1092-1100.

44. Karayan L, Hong SS, Gay B, Tournier J, Dangeac AD, Boulanger P. Structural and functional determinants in adenovirus type 2 penton base recombinant protein. J. Virol. 1997;71(11):8678-8689.

45. Green M, Loewenstein PM. Autonomous functional domains of chemically synthesized human immunodeficiency virus tat trans-activator protein. Cell 1988;55(6):1179-88.

46. Frankel AD, Pabo CO. Cellular uptake of the tat protein from human immunodeficiency virus. Cell 1988;55(6):1189-93.

47. Ho A, Schwarze SR, Mermelstein SJ, Waksman G, Dowdy SF. Synthetic protein transduction domains: enhanced transduction potential in vitro and in vivo. Cancer Res 2001;61(2):474-7.

48. Mai JC, Shen H, Watkins SC, Cheng T, Robbins PD. Efficiency of protein transduction is cell type-dependent and is enhanced by dextran sulfate. J Biol Chem 2002;277(33):30208-18.

49. Morris MC, Depollier J, Mery J, Heitz F, Divita G. A peptide carrier for the delivery of biologically active proteins into mammalian cells. Nat Biotechnol 2001;19(12):1173-6.

50. Barton ES, Forrest JC, Connolly JL, Chappell JD, Liu Y, Schnell FJ, et al. Junction adhesion molecule is a receptor for reovirus. Cell 2001;104(3):441-51.

51. Casjens S. Principles of virion structure, function and assembly. In: Chiu W, Burnett RM, Garcea RL, editors. Structural biology of viruses. Oxford: Oxford University Press; 1997. p. 3-37.

52. Bruder JT, Kovesdi I. Adenovirus Infection Stimulates the Raf/Mapk Signaling Pathway and Induces Interleukin-8 Expression. Journal of Virology 1997;71(1):398-404.

53. Suomalainen M, Nakano MY, Boucke K, Keller S, Greber UF. Adenovirus-activated PKA and p38/MAPK pathways boost microtubule-mediated nuclear targeting of virus. Embo J 2001;20(6):1310-1319.

54. Suomalainen M, Nakano MY, Boucke K, Keller S, Stidwill RP, Greber UF. Microtubule-dependent minus and plus end-directed motilities are competing processes for nuclear targeting of adenovirus. J. Cell Biol. 1999;144:657-672.

55. Nakano MY, Greber UF. Quantitative microscopy of fluorescent adenovirus entry. J. Struct. Biol. 2000;129:57-68.

56. Weber J. Genetic analysis of adenovirus type 2. III. Temperature sensitivity of processing of viral proteins. J. Virol. 1976;17:462-471.

57. Greber UF, Webster P, Weber J, Helenius A. The role of the adenovirus protease in virus entry into cells. EMBO J. 1996;15:1766-1777.

58. Whyte P, Buchkovich KJ, Horowitz JM, Friend SH, Raybuck M, Weinberg RA, et al. Association between an oncogene and an antioncogene: the Adenovirus E1A proteins bind to the retinoblastoma gene product. Nature 1988;334:124-129.

59. Baum SG, Horwitz MS, J.V. Maizel J. Studies of the mechanism of enhancement of human adenovirus infection in monkey cells by simian virus 40. J. Virol. 1972;10:211-219.

60. Fender P, Kidd AH, Brebant R, Oberg M, Drouet E, Chroboczek J. Antigenic sites on the receptor-binding domain of human adenovirus type 2 fiber. Virology 1995;214(1):110-7.

61. Berger EG, Aegerter E, Mandel T, Hauri HP. Monoclonal antibodies to soluble, human milk galactosyltransferase (lactose synthase A protein). Carbohydr Res 1986;149(1):23-33.

62. Greber UF, Suomalainen M, Stidwill RP, Boucke K, Ebersold M, Helenius A. The role of the nuclear pore complex in adenovirus DNA entry. EMBO J. 1997;16:5998-6007.

Figure Legends

Fig. 1: Pb is released from transiently transfected cells and associates with neighboring cells.

A549 cells were transfected with the Pb expression plasmid SK5.5 using Lipofectamin (a, a') or $CaPO_4$ precipitation (b, b'), fixed at 30 or 60 h p.t., respectively, and immunostained for Pb using the pAb R2. DIC images are shown in panels a and b. Bar = 50 µm.

Fig. 2: Export of Pb from cells infected with wt or mutant Ad2 occurs in various cell types.

A) A549 cells were infected with wt Ad2 at low moi (one of 40 infected cells) and fixed at the indicated time points p.i.. Pb was visualized by immunostaining using the pAb R2.

B) KB and HeLa cells were infected with wt Ad2 at low moi and Pb localization was visualized at 20 or 25 h p.i. as described above.

C) Pb export is unaffected by various deletions in the Ad2 genome. A549 cells were infected with the E3 14.7 K mutant Ad2-dl762 (a, a'), the ADP mutant Ad2-dl712 (b, b') or with the protease-defective ts1-Ad2 mutant (c, c') for 30 h and immunostained for Pb using pAb R2.

D) A549 cells were infected with wt Ad2 for 30 h, and Pb was visualized by immunostaining with the pAb 591. All bars = 50 µm.

Fig. 3: Pb is not recovered from the medium of infected cells up to 30 h p.i..

A) A549 cells (3×10^5) were infected with Ad2 (moi 100, cold synchronization) or not infected in protein-free Turbodoma medium for 0, 21 and 32 h (warming). The medium (0.3 ml equivalent to 10^5 cells) was briefly centrifuged at 3'000 x g, concentrated by

precipitation with trichloro-acetic acid, dissolved in SDS-sample buffer and analyzed by SDS 12%-PAGE and Western blotting with antibodies against penton base (R2) and interleukin 6 (IL-6). Note the absence of Pb in the supernatants, but the presence of IL-6 in both Ad2 infected and noninfected supernatants. Corresponding lysates of 10^4 cells were prepared in hot SDS and analyzed together with the supernatants (cells). * indicates the protein of interest.

B) A549 cells ($3x10^5$) were infected with Ad2 at moi 200 by cold synchronization or were not infected for 0, 10, 23 and 31 h in DMEM-BSA at 37°C (see 32). The medium was centrifuged briefly at 3'000 x g and Pb immuncomplexes were collected with the R2 antibody and protein G-Sepharose. 10^5 cell equivalents were analyzed by SDS-PAGE and Western blotting using R2. Note that Pb was not collected from these supernatants, but that it was detected in immunprecipitates of 10^5 infected infected cell equivalents. The sensitivity of our Western blot was about 0.1 µg Pb, as indicated by purified Ad2.

C) The supernatant of Ad2 infected or noninfected A549 cells was collected at 41 h p.i., centrifuged to remove Ad particles and applied to noninfected A549 cells at 37°C for 6 h, followed by immunofluorescence analysis of the acceptor cells using the Pb-specific R2 antibody and DAPI and DIC imaging (panels d-f and g-l). Note the increase of Pb staining on the acceptor cells excluding the nucleus indicated by DAPI staining. As an additional control, A549 cells were infected with purified Ad2 at moi 200 for 6 h after cold synchronization (panels a-c). Note the nuclear enrichment of Pb derived from Ad2 particles. The fluorescence images of Pb and DAPI are the projections of all the optical confocal laser scanning microscopy sections across one layer of cells, taken at 0.5 µm intervals.

Fig. 4: Quantification of Pb release from cells infected with Ad2.

A) Pb was immunostained with the pAb R2 30 h p.i.. The signal intensities within the infected cell (c), the entire image (a) and a region with background signal (b) were

measured by the MetaMorph software package. On average 46.6 % (n = 18, Stdev = 13.7 %) of the signal was found outside of the donor cell. Bar = 50 µm.

B) No evidence of Pb degradation. A549 cells grown on 30 mm culture dishes were transfected with a Pb expression plasmid for 19 h (lane 1), 29 h (lane 2) 43 h (lane 3), 52 h (lane 4), 69 h (lane 5) or infeced with wt Ad2 (lane 6) or left nontransfected (lane 7). Cells were extracted with SDS and lysates analyzed by SDS-PAGE and Coomassie blue staining (a) as well as Western blotting with the anti-Pb pAb R2 (b).

Fig 5: The plasma membrane of the Ad infected cells is impermeable to Trypan Blue and eGFP but allows the exit of Pb in the absence of Golgi membranes.

A) 911 cells (expressing Ad E1A and E1B proteins) were infected with Ad5-eGFP at a low MOI for 30 hr. Trypan Blue was added to live cells for 10 min, followed by DIC imaging (a), fixation and eGFP analysis by fluorescence microscopy (b). Arrows indicate Trypan Blue positive (i.e. permeable) cells. Note that the infected cells are not permeable to Trypan Blue.

B) 911 cells were infected with Ad5-eGFP, fixed at 30 h p.i. and processed for immunofluorescence using the anti-Pb pAb R2 (a''), eGFP analysis (a') and DIC (a).

C) Pb export does not involve the Golgi apparatus. A549 cells were infected with wt Ad2 (a, a', a'' and b, b', b'') or transfected with a Pb expression plasmid (c-c'' and d-d''), incubated for 18 h and fixed (a-a'' and c-c''). Parallel samples were further treated with BFA (2.5 µg/ml) until 30 h p.i. or p.t. and fixed (b-b'' and d-d''). Samples were stained with pAb R2 (Pb, a'-d') or with a mAb anti-GalT (a''-d'') and analyzed by indirect immunofluorescence microscopy including DIC imaging (a-d). All bars = 50 µm.

Fig 6: Fiber spreading requires Pb and occurs in different cell types.

A) KB and HeLa cells were infected with wt Ad2 and stained after indicated time points by indirect immunofluorescence with the mAb 6A4 against the knob domain of Ad2 fiber or

the pAb R70 directed to hexon. Export of fiber but not hexon was detected in A549 cells (a' and b') and fiber was also found outside HeLa cells (c) and KB cells (d) at the indicated time points p.i..

B) A549 cells were transfected with fiber expressing plasmid (SK6.10) using Lipofectamin and processed for immunofluorescence against fiber using mAb 6A4 30 h p.t. (a'). Importantly, fiber spreading was not observed at later time points, but was clearly visible in cells co-transfected with Pb plasmid (SK5.5, panel b'), similar to the spreading of Pb which was visualized with pAb R2 (b''). DIC images are shown in panels a and b. All bars = 50 µm.

Fig 7: Exported fiber and Pb are found in the periphery of the recipient cells.

A549 cells were infected with wt Ad2 for 30 h and double immuno-stained for Pb (a) and fiber (b) using the pAb R2 and the mAb 6A4, respectively. Single CLSM sections across the lower mid of the infected cell (a-c) and the projection of the entire set of optical slices (d) are shown. The merged Pb and fiber images indicate potential colocalization of Pb and fiber (c, d). Bar = 50 µm.

Fig. 1 Trotman et al.

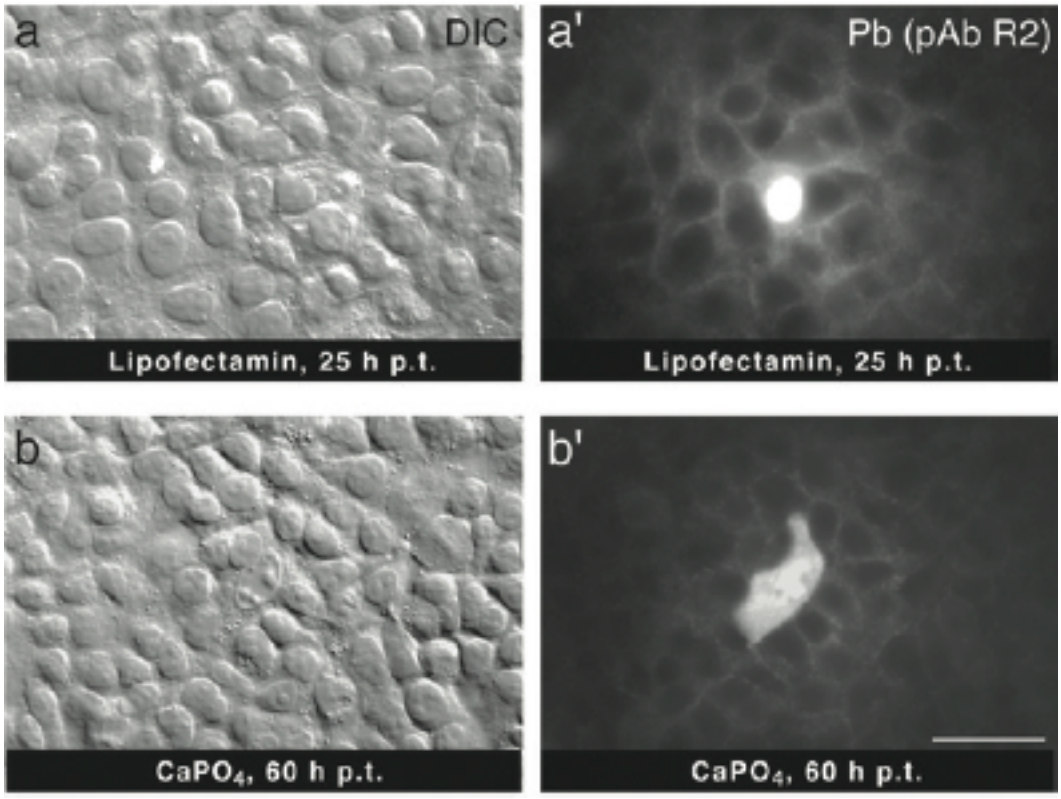

Fig. 2 Trotman et al.

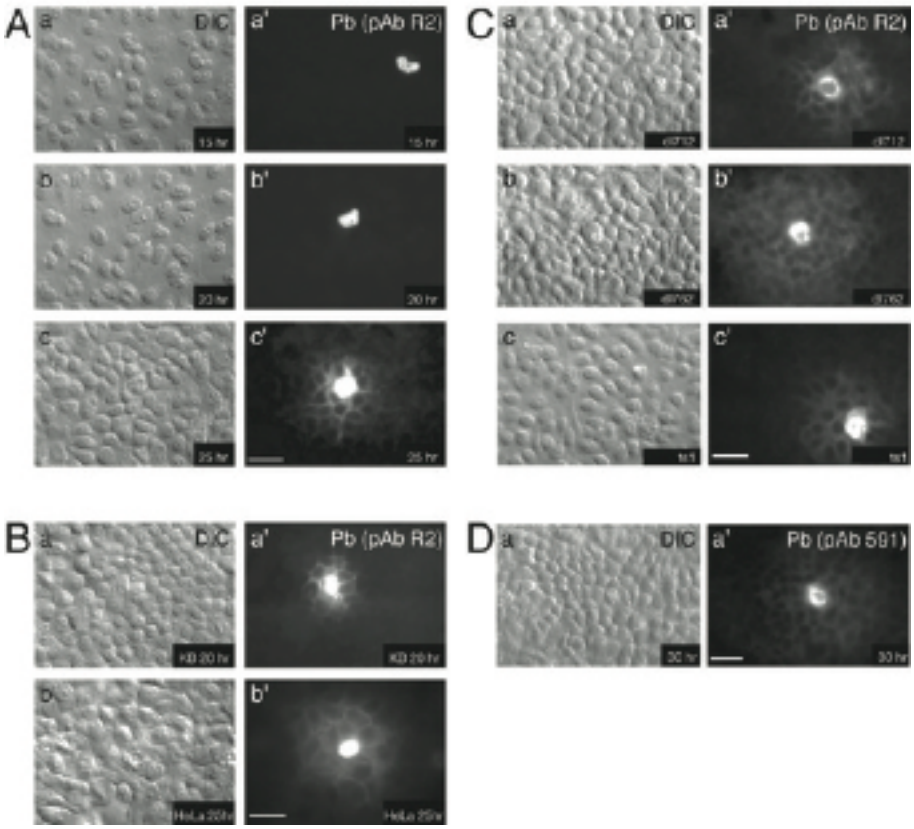

Fig. 3 Trotman et al.

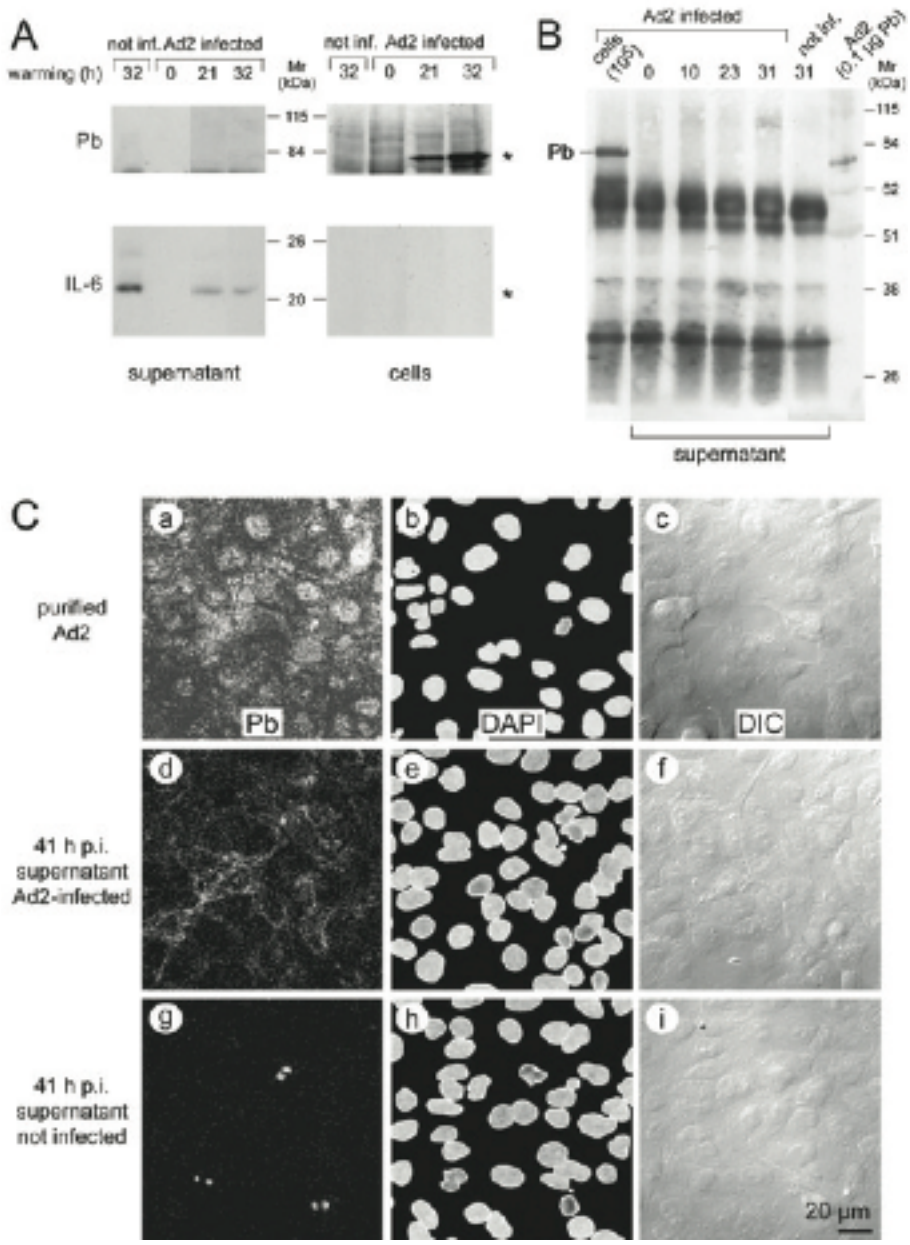

Fig. 4 Trotman et al.

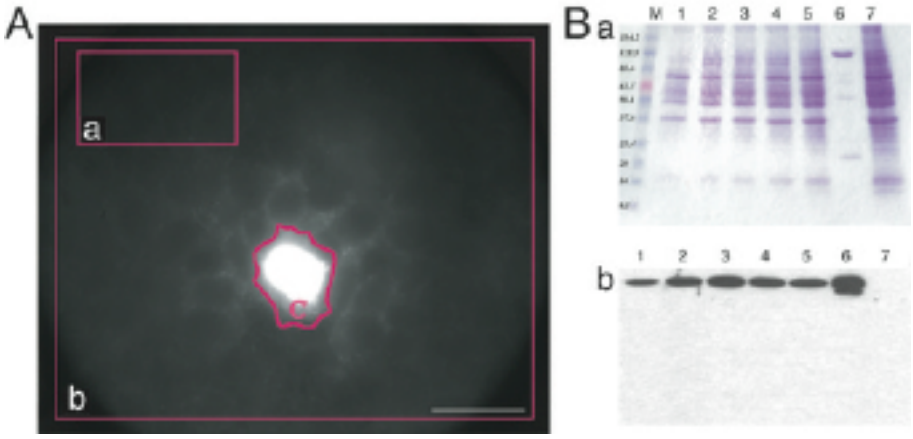

Fig. 5 Trotman et al.

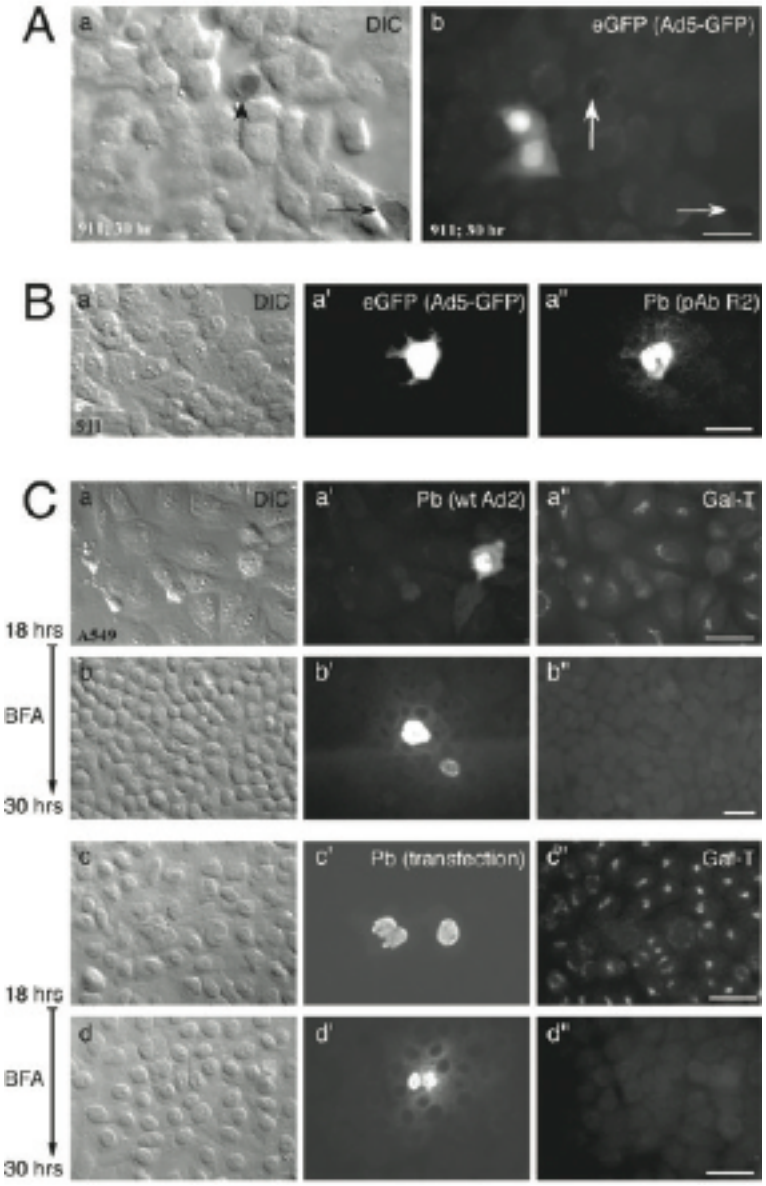

Fig. 6 Trotman et al.

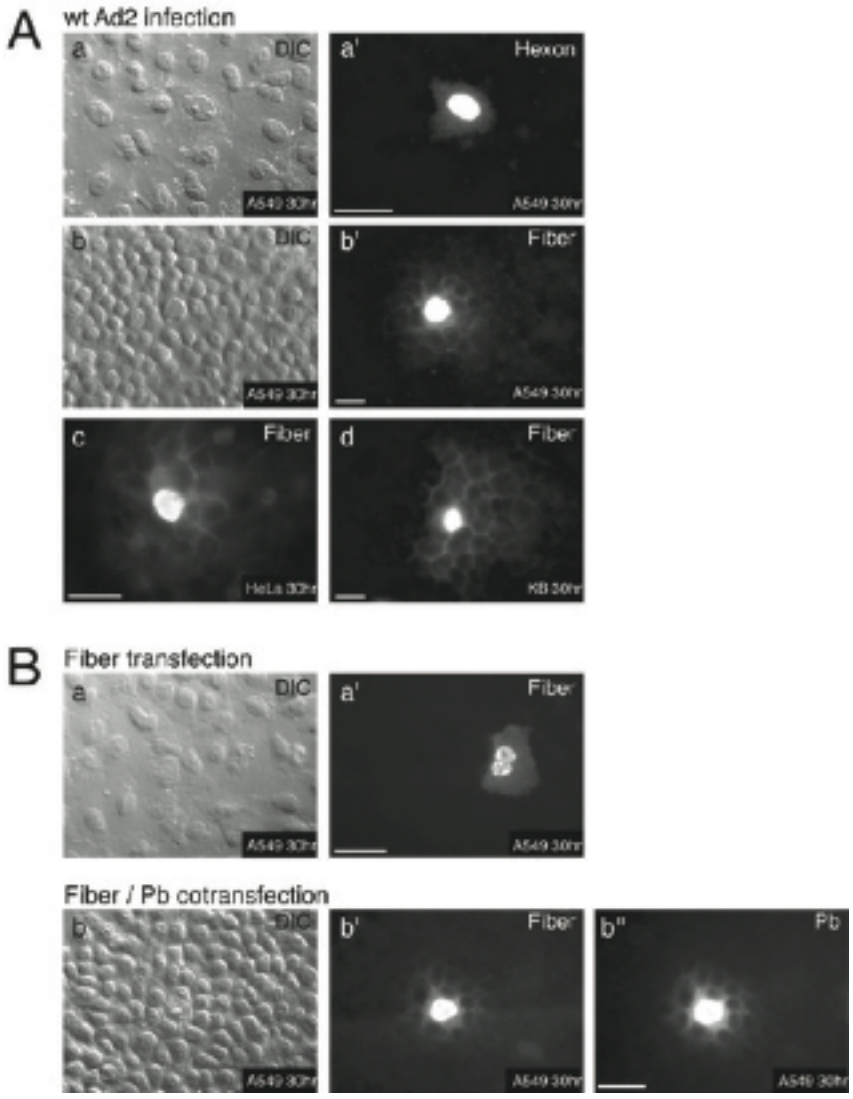

Fig. 7 Trotman et al.